

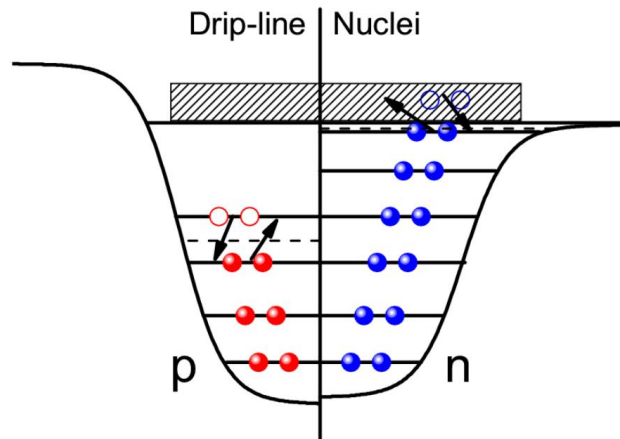
Nuclear mass table in deformed relativistic continuum Hartree-Bogoliubov theory

EunJin In,
Seung-Woo Hong, CDFT collaboration

Sungkyunkwan university

01 Introduction

- Continuum and pairing correlations play a critical role in exotic nuclei.

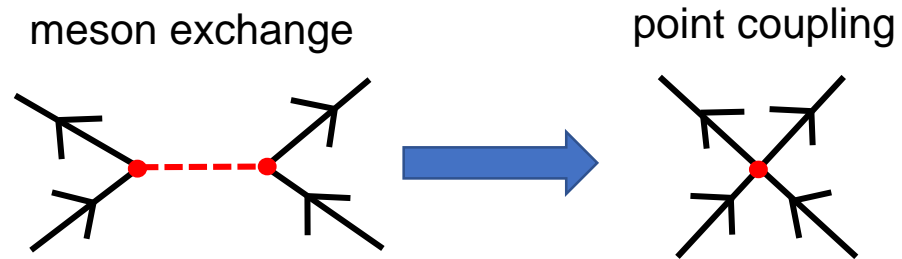


- Relativistic continuum Hartree-Bogoliubov (RCHB) theory
 - treat pairing correlations in the presence of the continuum properly
 - RCHB theory is used to explore nuclear mass, especially nucleon drip lines by assuming spherical symmetry
 - Calculations for $8 \leq Z \leq 120$ isotopes was completed¹⁾
- Deformed RHB (DRHB) theory in continuum
 - assume axial symmetry
 - Investigate deformation effects on the neutron drip line

01 Introduction

- Covariant density functional theory

- Finite-range meson-exchange
 - Zero-range point-coupling



- Our purpose

- effect of deformation on position of neutron drip line with DRHB theory
 - Ar isotopes as examples

02 Relativistic continuum Hartree-Bogoliubov theory

- Lagrangian density of the point-coupling model¹⁾

$$\mathcal{L} = \mathcal{L}^{free} + \mathcal{L}^{4f} + \mathcal{L}^{hot} + \mathcal{L}^{der} + \mathcal{L}^{em}$$

where

$$\mathcal{L}^{free} = \bar{\psi} (i\gamma_\mu \partial^\mu - m) \psi$$

$$\mathcal{L}^{4f} = -\frac{1}{2} \alpha_S (\bar{\psi} \psi)(\bar{\psi} \psi) - \frac{1}{2} \alpha_V (\bar{\psi} \gamma_\mu \psi)(\bar{\psi} \gamma^\mu \psi) - \frac{1}{2} \alpha_{TV} (\bar{\psi} \vec{\tau} \gamma_\mu \psi)(\bar{\psi} \vec{\tau} \gamma^\mu \psi)$$

$$\mathcal{L}^{hot} = -\frac{1}{3} \beta_S (\bar{\psi} \psi)^3 - \frac{1}{4} \gamma_S (\bar{\psi} \psi)^4 - \frac{1}{4} \gamma_V [(\bar{\psi} \gamma_\mu \psi)(\bar{\psi} \gamma^\mu \psi)]^2$$

$$\begin{aligned} \mathcal{L}^{der} = & -\frac{1}{2} \delta_S \partial_\nu (\bar{\psi} \psi) \partial^\nu (\bar{\psi} \psi) - \frac{1}{2} \delta_V \partial_\nu (\bar{\psi} \gamma_\mu \psi) \partial^\nu (\bar{\psi} \gamma^\mu \psi) \\ & - \frac{1}{2} \delta_{TV} \partial_\nu (\bar{\psi} \vec{\tau} \gamma_\mu \psi) \partial^\nu (\bar{\psi} \vec{\tau} \gamma_\mu \psi) \end{aligned}$$

$$\mathcal{L}^{em} = -\frac{1}{4} F^{\mu\nu} F_{\mu\nu} - e \frac{1 - \tau_3}{2} \bar{\psi} \gamma^\mu \psi A_\mu$$

02 Relativistic continuum Hartree-Bogoliubov theory

- Relativistic Hartree-Bogoliubov (RHB) equation¹⁾

$$\begin{pmatrix} h_D - \lambda & \Delta \\ -\Delta^* & -h_D^* + \lambda \end{pmatrix} \begin{pmatrix} U_k \\ V_k \end{pmatrix} = E_k \begin{pmatrix} U_k \\ V_k \end{pmatrix}$$

- Dirac Hamiltonian

$$h_D = \boldsymbol{\alpha} \cdot \boldsymbol{p} + \beta(M + S(r)) + V(r)$$

where scalar and vector potentials

$$S(r) = \alpha_S \rho_S + \beta_S \rho_S^2 + \gamma_S \rho_S^3 + \delta_S \Delta \rho_S$$

$$V(r) = \alpha_V \rho_V + \gamma_V \rho_V^3 + \delta_V \Delta \rho_V + eA_0 + \alpha_{TV} \tau_3 \rho_{TV} + \delta_{TV} \tau_3 \Delta T_V$$

with local densities

$$\rho_S = \sum_{k>0} \bar{V}_k(r) V_k(r), \quad \rho_V = \sum_{k>0} V_k^+(r) V_k(r),$$

$$\rho_{TV} = \sum_{k>0} V_k^+(r) \tau_3 V_k(r)$$

02 Relativistic continuum Hartree-Bogoliubov theory

- The point-coupling constants of PC-PK1 set¹⁾.

Coupling constant	Value	Dimension
α_s	$-3.962\ 91 \times 10^{-4}$	MeV^{-2}
β_s	8.6653×10^{-11}	MeV^{-5}
γ_s	$-3.807\ 24 \times 10^{-17}$	MeV^{-8}
δ_s	$-1.091\ 08 \times 10^{-10}$	MeV^{-4}
α_v	2.6904×10^{-4}	MeV^{-2}
γ_v	$-3.642\ 19 \times 10^{-18}$	MeV^{-8}
δ_v	$-4.326\ 19 \times 10^{-10}$	MeV^{-4}
α_{tv}	$2.950\ 18 \times 10^{-5}$	MeV^{-2}
δ_{tv}	$-4.111\ 12 \times 10^{-10}$	MeV^{-4}

fitted to observables of 60 selected spherical nuclei,
including the binding energies, charge radii, and empirical pairing gaps.

02 Relativistic continuum Hartree-Bogoliubov theory

- Relativistic Hartree-Bogoliubov equation¹⁾

$$\begin{pmatrix} h_D - \lambda & \Delta \\ -\Delta^* & -h_D^* + \lambda \end{pmatrix} \begin{pmatrix} U_k \\ V_k \end{pmatrix} = E_k \begin{pmatrix} U_k \\ V_k \end{pmatrix}$$

- Pairing potential

with a density-dependent delta pairing force

$$V^{pp}(\mathbf{r}, \mathbf{r}') = \frac{V_0}{2} (1 - P^\sigma) \delta(\mathbf{r} - \mathbf{r}') (1 - \frac{\rho(\mathbf{r})}{\rho_{sat}})$$

with the saturation density $\rho_{sat} = 0.152 \text{ fm}^{-3}$,
and the pairing force strength $V_0 = -380.0 \text{ MeV} \cdot \text{fm}^3$

03 Deformed RHB theory (DRHB) in continuum

- Quasiparticle wave functions U and V are expanded in terms of spherical Dirac spinors $\varphi_{n\kappa m}(\mathbf{r}sp)$

$$U_k(\mathbf{r}sp) = \sum_{n\kappa} u_{k,(n\kappa)}^{(m)} \varphi_{n\kappa m}(\mathbf{r}sp)$$

$$V_k(\mathbf{r}sp) = \sum_{n\kappa} v_{k,(n\kappa)}^{(m)} \bar{\varphi}_{n\kappa m}(\mathbf{r}sp)$$

The basis wave function reads $\varphi_{n\kappa m}(\mathbf{r}s) = \frac{1}{r} \begin{pmatrix} iG_{n\kappa}(r)Y_{jm}^l(\Omega s) \\ -F_{n\kappa}(r)Y_{jm}^{\tilde{l}}(\Omega s) \end{pmatrix}$

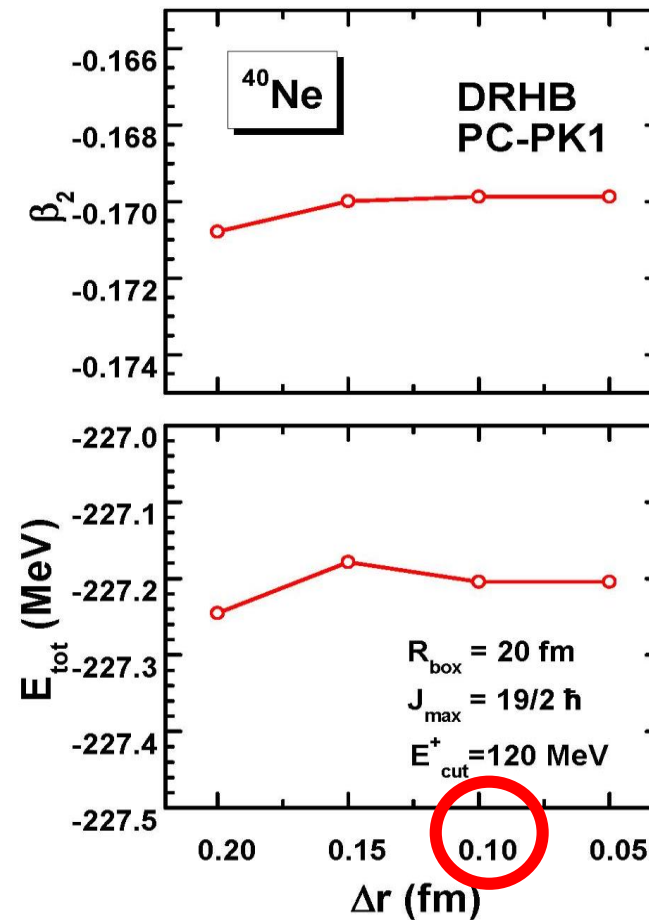
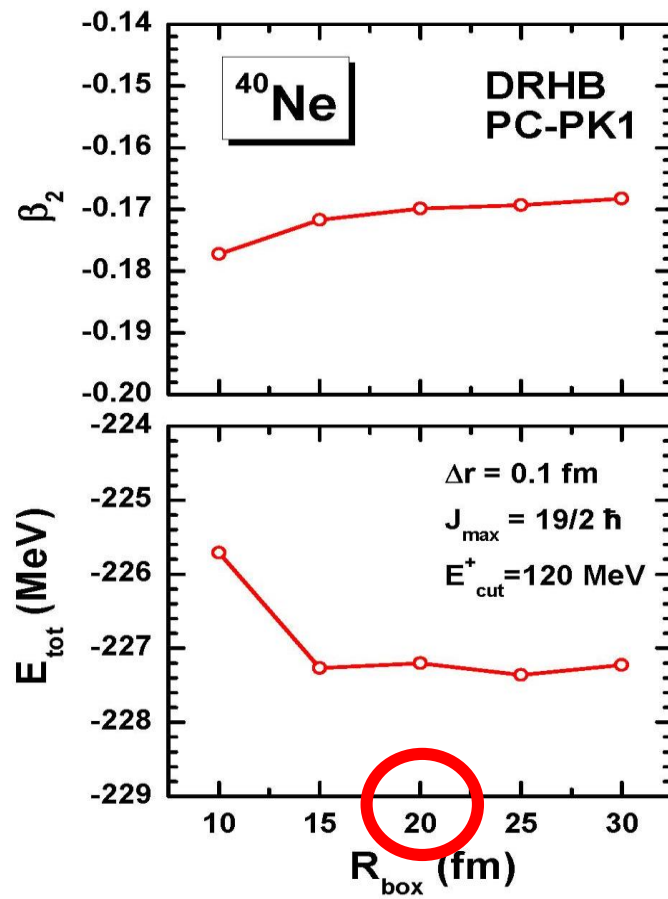
- For axially deformed nuclei**, potential $S(r)$ and $V(r)$ and densities are expanded in terms of the Legendre polynomials

$$f(\mathbf{r}) = \sum_{\lambda} f_{\lambda}(r) P_{\lambda}(\cos \theta), \lambda = 0, 2, 4, \dots$$

$$\text{with } f_{\lambda}(r) = \frac{2\lambda + 1}{4\pi} \int d\Omega f(\mathbf{r}) P_{\lambda}(\Omega).$$

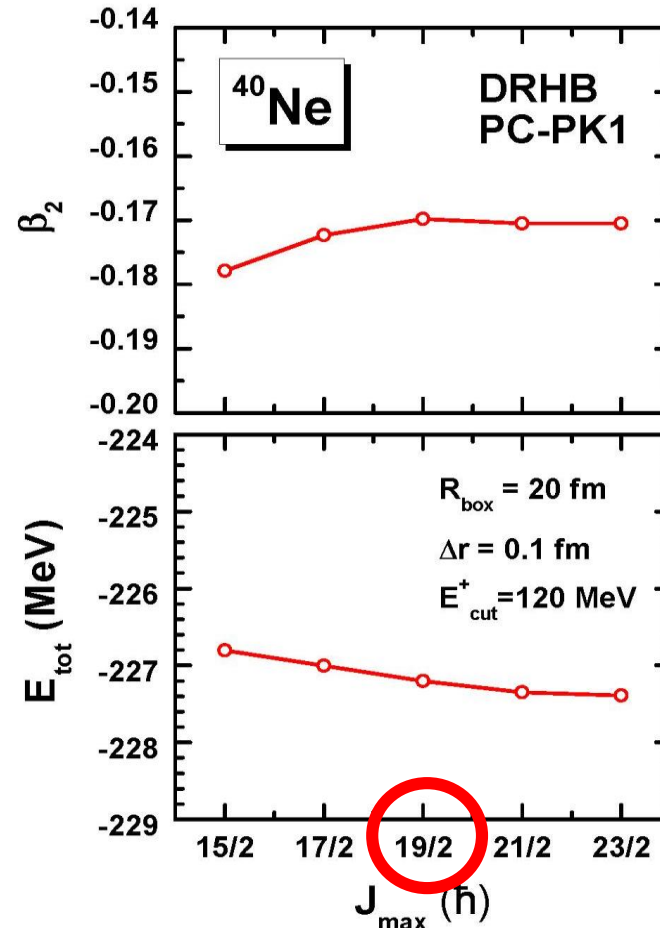
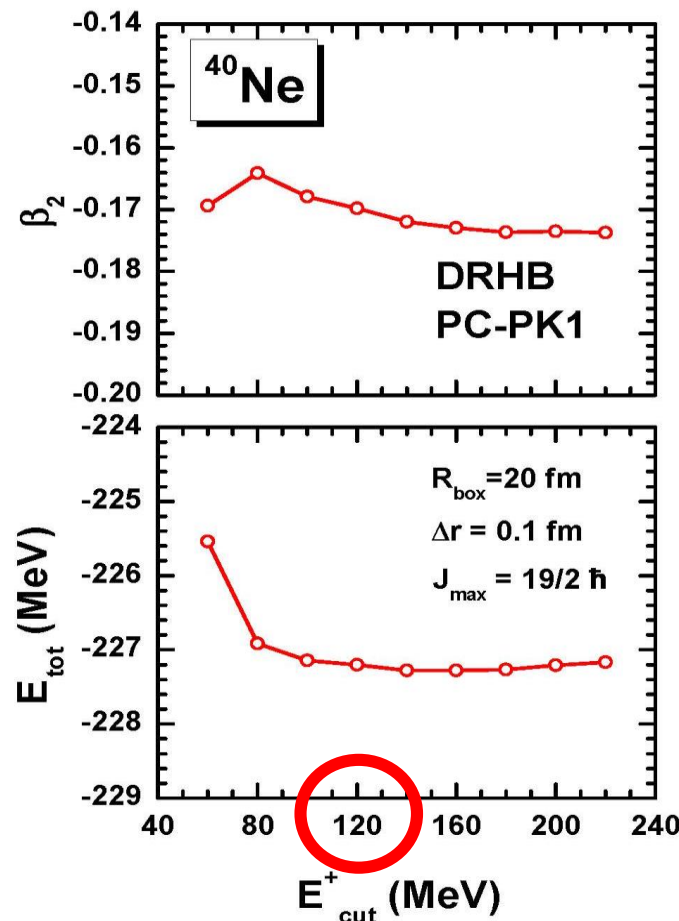
04 Numerical details: box size, mesh size

- Numerical parameters in calculation
 - box size, mesh size



04 Numerical details: energy and angular momentum cutoff

- Numerical parameters in calculation
 - energy cutoff, angular momentum cutoff

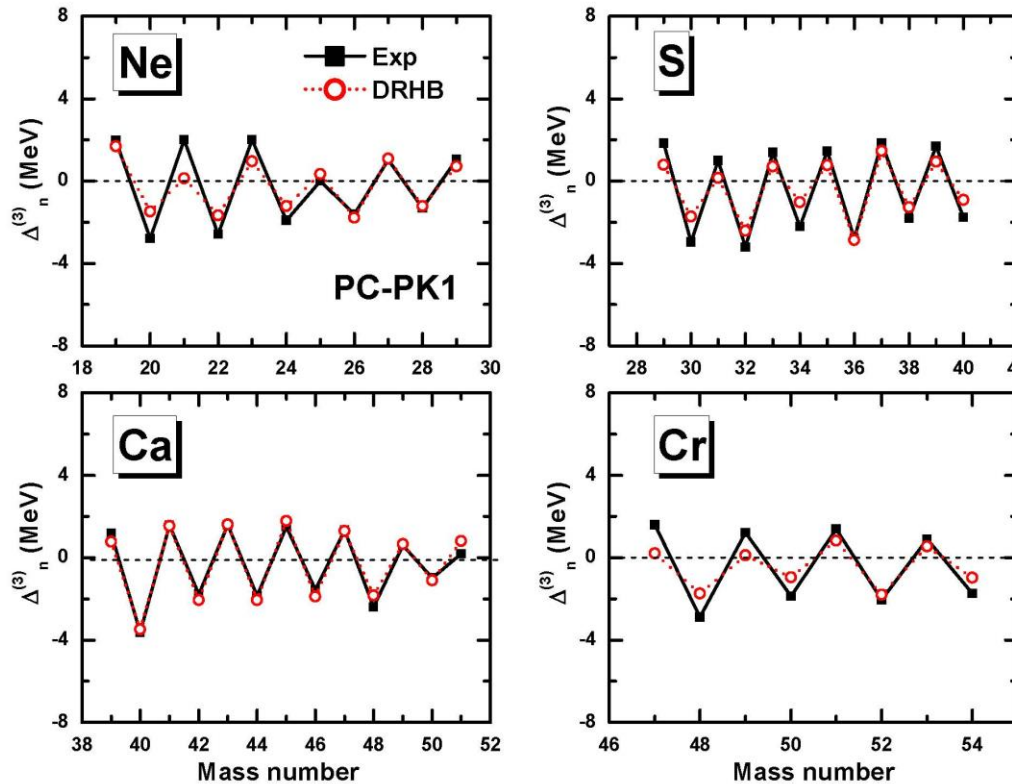


04 Numerical details: Pairing strength

- Density-dependent delta pairing force

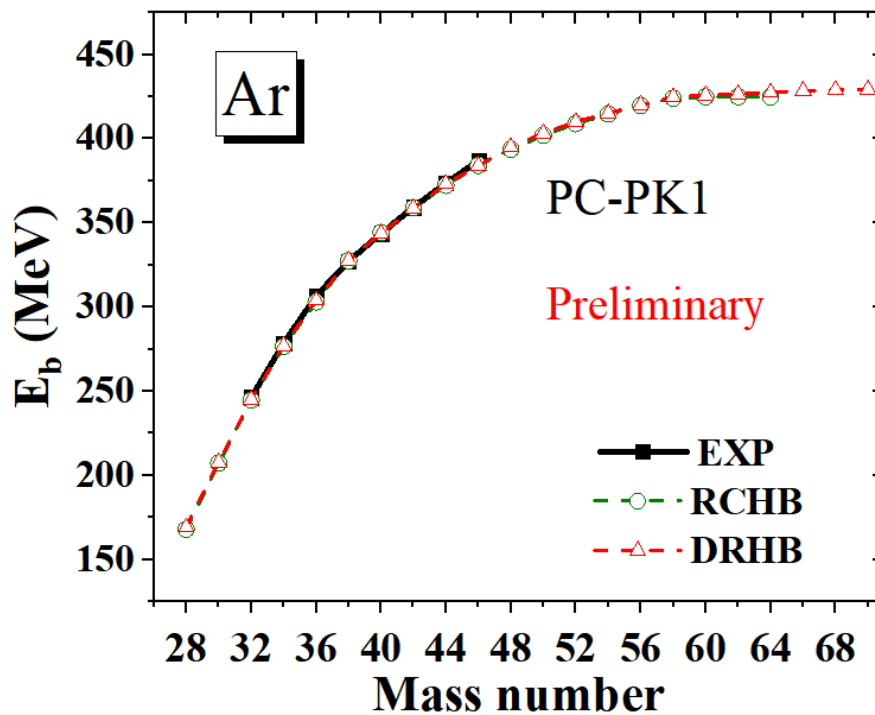
$$V^{pp}(\mathbf{r}, \mathbf{r}') = \frac{V_0}{2} (1 - P^\sigma) \delta(\mathbf{r} - \mathbf{r}') (1 - \frac{\rho(\mathbf{r})}{\rho_{sat}})$$

with the saturation density $\rho_{sat} = 0.152 \text{ fm}^{-3}$,
and the pairing force strength $V_0 = -380.0 \text{ MeV} \cdot \text{fm}^3$



05 Results

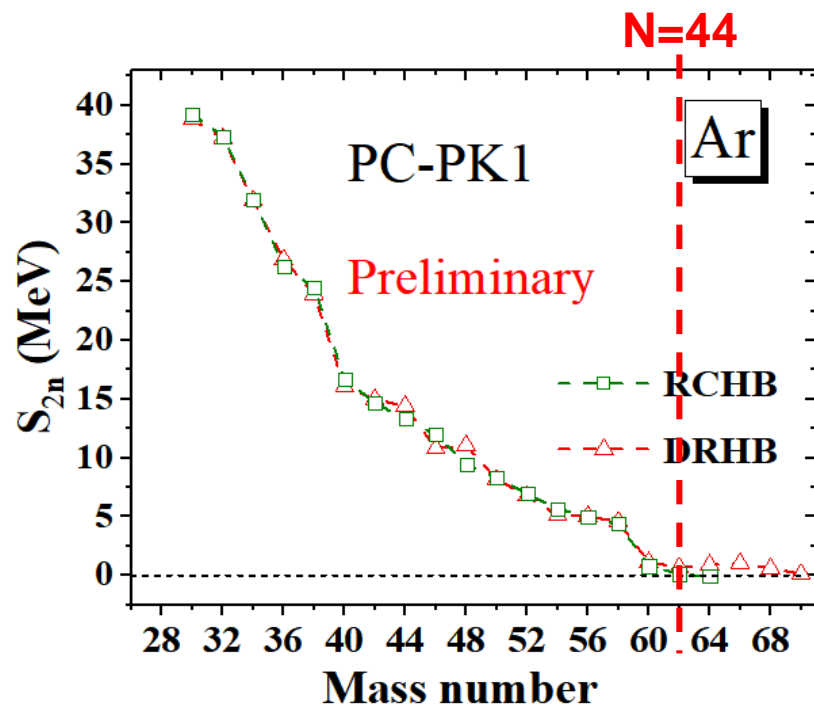
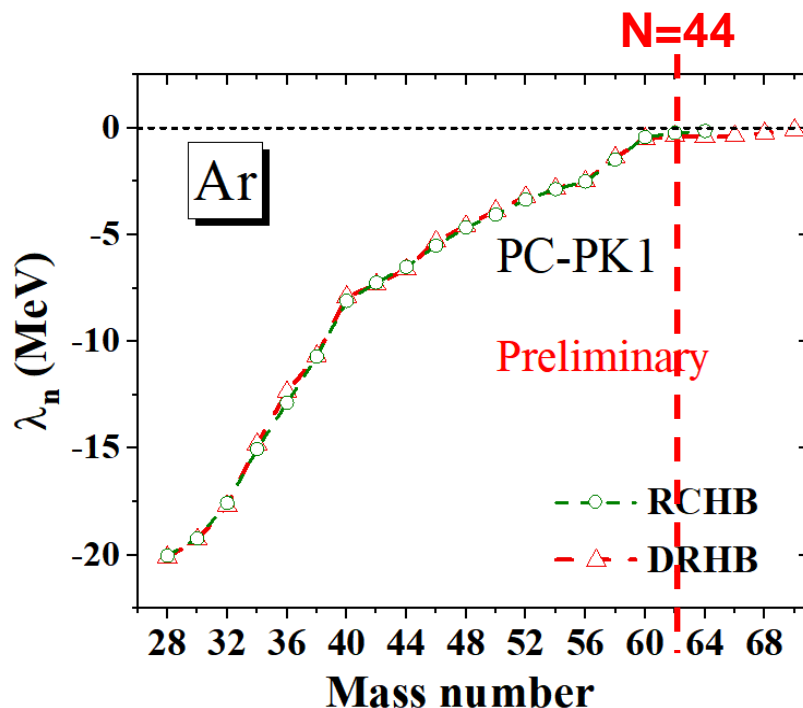
- Comparison of binding energies between experimental values¹⁾ and calculations by using RCHB and DRHB theory + PC-PK1



Both models reproduce well the experiment

05 Results

- Comparison of Fermi energy and two neutron separation energy between calculations by using RCHB and DRHB theory + PC-PK1



In the case of Ar isotopes, the neutron drip-line nucleus from ^{62}Ar in the RCHB to ^{70}Ar in the DRHB calculations

05 Results

- Compare with **FRDM**(finite range droplet model)¹⁾,
the neutron drip-line nucleus predicted by **RCHB**²⁾ theory has more neutrons.

Element (Z)	More N	Element(Z)	More N
O (8)	2	Ca (20)	10
Ne (10)	10	Mo (42)	12
Mg (12)	6	Ru (44)	10
Si (14)	6	Pd (46)	13
S (16)	6	Cd (48)	6

Preliminary

- The neutron number of the most neutron-rich even-even nuclei predicted to be bound in the **RCHB** and **DRHB** theory, in comparing with the calculations without pairing correlations

Preliminary

Element (Z)	Neutron number			Element(Z)	Neutron number		
	No pairing	RCHB	DRHB		No pairing	RCHB	DRHB
O (8)	20	20	20	Ca (20)	40	60	58
Ne (10)	20	32	30	Mo (42)	112	112	78
Mg (12)	34	34	34	Ru (44)	112	112	114
Si (14)	34	38	38	Pd (46)	112	118	118
S (16)	40	40	40	Cd (48)	112	126	124
Ar (18)	40	44	52				

06 Mass table with DRHB theory

- Example of mass table with DRHB theory

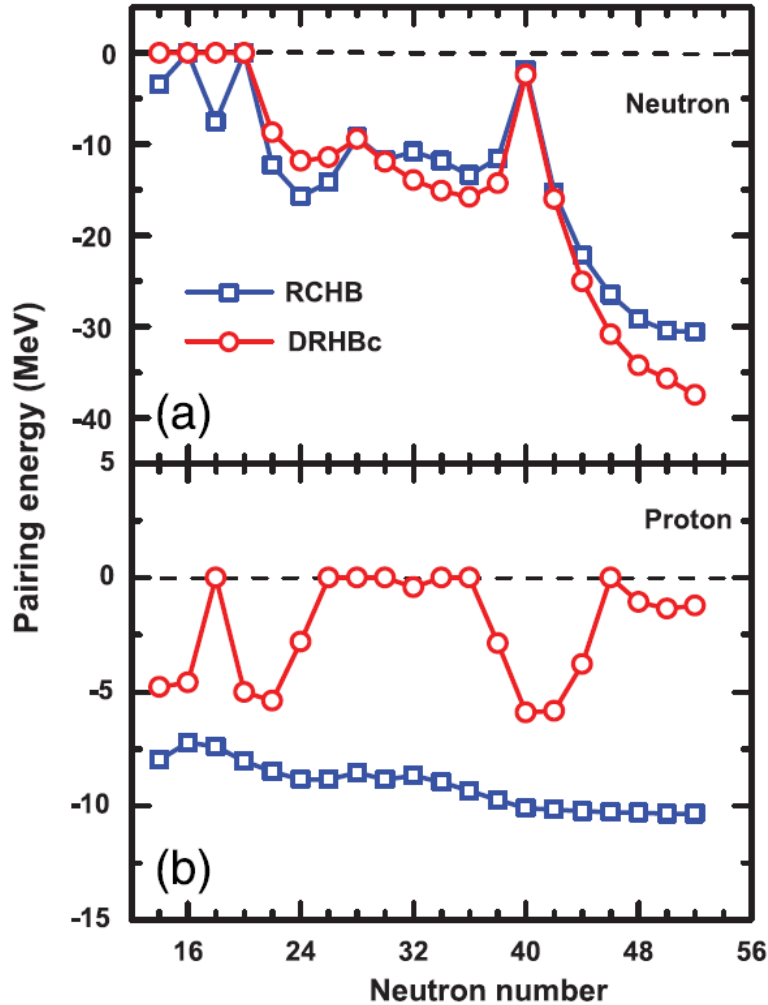
- Z=18 (Ar) isotopes Preliminary

07 Summary

- We studied on deformation effect on the position of neutron drip line with DRHB + PC-PK1 calculation in continuum.
- We compared the neutron number of the even-even nuclei predicted to be bound in the RCHB and DRHB theory, taking Ar isotopes as an example.
- We can find that the deformation would affect the position of neutron drip line.
- Future work
 - Additional calculations for other isotopes to study on deformation effects of neutron drip line position
 - Study on other characteristic of deformed nuclei such as decoupling shape of halo and core densities

Thank you

00 Pairing energies for argon isotopic chain



00 Mass table calculated by RCHB theory

■ Mass table calculated by RCHB theory

Atomic Data and Nuclear Data Tables 121–122 (2018) 1–215



The limits of the nuclear landscape explored by the relativistic continuum Hartree–Bogoliubov theory



X.W. Xia^a, Y. Lim^{b,c}, P.W. Zhao^{d,e}, H.Z. Liang^f, X.Y. Qu^{a,g}, Y. Chen^{d,h}, H. Liu^d, L.F. Zhang^d, S.Q. Zhang^d, Y. Kim^c, J. Meng^{d,a,i,*}

^a School of Physics and Nuclear Energy Engineering, Beihang University, Beijing 100191, China

^b Cyclotron Institute, Texas A&M University, College Station, TX 77843, USA

^c Rare Isotope Science Project, Institute for Basic Science, Daejeon 305-811, Republic of Korea

^d State Key Laboratory of Nuclear Physics and Technology, School of Physics, Peking University, Beijing 100871, China

^e Physics Division, Argonne National Laboratory, Argonne, IL 60439, USA

^f RIKEN Nishina Center, Wako 351-0198, Japan

^g School of Mechatronics Engineering, Guizhou Minzu University, China

^h Institute of materials, China Academy of Engineering Physics, Sichuan, 621907, China

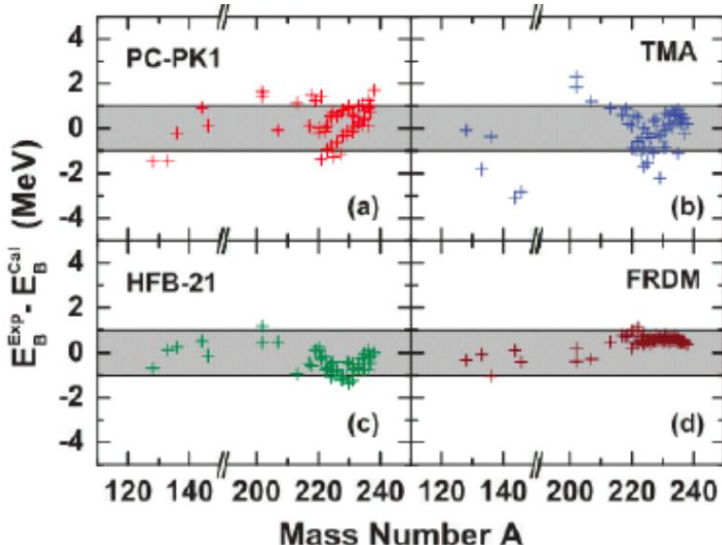
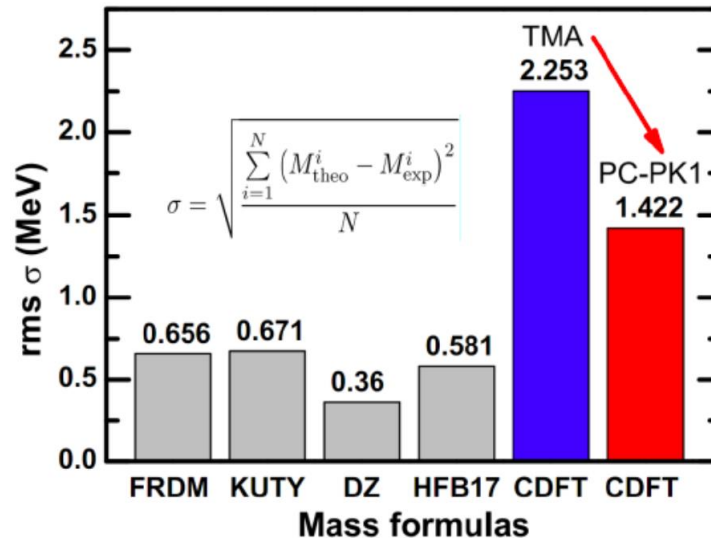
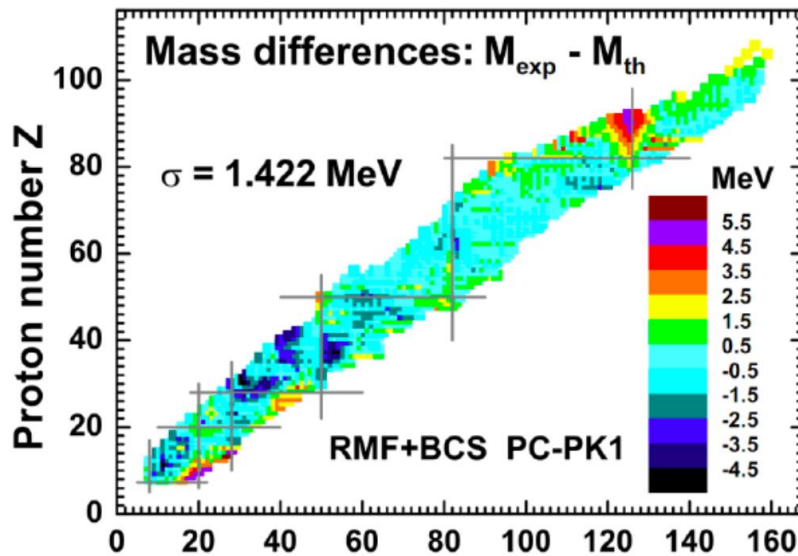
ⁱ Department of Physics, University of Stellenbosch, Stellenbosch, South Africa

Table 1

Ground-state properties of nuclei calculated by RCHB theory with PC-PK1, in comparison with the available data of masses and charge radii. In addition, the data labeled with underline means the nucleus is unbound.

A	N	$E_b^{\text{Cal.}}$ (MeV)	$E_b^{\text{Exp.}}$ (MeV)	$E_b^{\text{Cal.}}/A$ (MeV)	$E_b^{\text{Exp.}}/A$ (MeV)	S_{2n} (MeV)	S_{2p} (MeV)	S_n (MeV)	S_p (MeV)	λ_n (MeV)	λ_p (MeV)	R_m (fm)	R_n (fm)	R_p (fm)	$R_c^{\text{Cal.}}$ (fm)	$R_c^{\text{Exp.}}$ (fm)	$j^\pi(P)$	$j^\pi(N)$
<i>Z = 8 (O)</i>																		
12	4	60.44	58.68	5.04	4.88					-19.45	<u>0.44</u>	2.738	2.335	2.919	3.027		0 ⁺	0 ⁺
13	5	77.81	75.56	5.99	5.81		17.38			-17.01	-0.99	2.619	2.373	2.762	2.876		0 ⁺	3/2 ⁻
14	6	101.86	98.73	7.28	7.05	41.42	24.05			-19.96	-1.34	2.465	2.238	2.621	2.741		0 ⁺	0 ⁺
15	7	112.81	111.96	7.52	7.46	34.99	10.95			-15.48	-5.43	2.599	2.537	2.652	2.770		0 ⁺	1/2 ⁻
16	8	127.29	127.62	7.96	7.98	25.43	14.48			-11.64	-7.83	2.638	2.626	2.649	2.768	2.701	0 ⁺	0 ⁺
17	9	132.48	131.76	7.79	7.75	19.67	5.19			-13.49	-9.79	2.690	2.733	2.642	2.760	2.695	0 ⁺	5/2 ⁺
18	10	141.63	139.81	7.87	7.77	14.34	9.15			-6.94	-11.79	2.736	2.807	2.644	2.763	2.775	0 ⁺	0 ⁺
19	11	145.27	143.76	7.65	7.57	12.79	3.64			-6.18	-13.50	2.792	2.896	2.642	2.760		0 ⁺	5/2 ⁺
20	12	153.16	151.37	7.66	7.57	11.54	7.89			-5.76	-15.10	2.842	2.964	2.649	2.767		0 ⁺	0 ⁺
21	13	156.04	155.18	7.43	7.39	10.77	2.88			-5.74	-16.16	2.935	3.096	2.653	2.771		0 ⁺	1/2 ⁺
22	14	162.91	162.03	7.41	7.36	9.75	6.87			-4.79	-18.54	2.955	3.111	2.659	2.777		0 ⁺	0 ⁺
23	15	166.49	164.77	7.24	7.16	10.45	3.58			-3.63	-19.61	3.001	3.173	2.650	2.768		0 ⁺	1/2 ⁺
24	16	170.90	168.95	7.12	7.02	7.99	4.41			-3.39	-20.52	3.082	3.268	2.672	2.789		0 ⁺	0 ⁺
25	17	172.02	168.18	6.88	6.73	5.53	1.12			-3.41	-23.79	3.169	3.370	2.692	2.809		0 ⁺	3/2 ⁺
26	18	175.10	168.86	6.73	6.49	4.20	3.08			-2.14	-22.36	3.230	3.428	2.732	2.847		0 ⁺	0 ⁺
27	19	175.57		6.50		3.56	0.47			-0.89	-23.36	3.310	3.516	2.760	2.874		0 ⁺	3/2 ⁺
28	20	178.02		6.36		2.92	2.45			-0.89	-23.36	3.370	3.576	2.790	2.903		0 ⁺	0 ⁺
σ																0.054		

00 Why adopt density functional PC-PK1?



A crucial test for covariant density functional theory against new and accurate mass measurement for 53 neutron-rich isotopes from Sn to Pa

- For 12 even-even nuclei, the theory agrees the data within about 600 keV.
- For 25 odd-A and 16 add-add nuclei, the rms values given by PC-PK1 are still within 1 MeV.

Zhao, Song, Sun, Geissel, Meng, Phys. Rev. C 86, 064323 (2012)